SUPPLEMENTARY MATERIALS: UNIFORM MULTIPENALTY REGULARIZATION FOR LINEAR ILL-POSED INVERSE PROBLEMS*

VILLIAM BORTOLOTTI†, GERMANA LANDI‡, AND FABIANA ZAMA‡

Introduction. This document presents the supplementary materials for the article titled "Uniform Multi-Penalty Regularization for Linear Ill-Posed Inverse Problems" by Villiam Bortolotti, Germana Landi, and Fabiana Zama. The supplementary materials provide extended discussions on one-dimensional test problems. After the description of the test problems and algorithmic settings in section SM1, low noise and high noise results are extensively discussed in sections SM2 and SM3 respectively.

SM1. One-dimensional test problems. Starting from a ground-truth signal $\mathbf{u}^* \in \mathbb{R}^N$, we generate the test problem by convolving it with a blurring operator $A \in \mathbb{R}^{M\times N}$ and then corrupting the blurred signal with additive Gaussian noise of level δ, i.e.

$$\mathbf{b} = \mathbf{y} + \text{noise}$$

where noise $= \delta\boldsymbol{\eta}\|\mathbf{y}\|$, with $\mathbf{y} = A\mathbf{u}^*$ and $\boldsymbol{\eta} \in \mathbb{R}^M$ a random normal vector with norm one. We consider two scenarios: a low-noise scenario corresponding to $\delta = 0.01$, and a high-noise scenario where $\delta = 0.1$. We define three test problems where each signal has different and progressively more complex features representing a challenge for the regularization functions.

- `T1` The signal $\mathbf{u}^* \in \mathbb{R}^{100}$ and the linear operator $A \in \mathbb{R}^{100\times 100}$ are obtained by the `heat` function from Hansen's Regularization Tools [SM1]. The ground truth $\mathbf{u}^*$, represented in Figure SM1 (left), is a sparse signal with mostly zero values except for a single peak quite close to the axes origin.
- `T2` The signal $\mathbf{u}^* \in \mathbb{R}^{404}$ (Figure SM1, center) has two narrow peaks over a flat area and a smooth rounded area. The operator A represents a Gaussian blur with a standard deviation of five.
- `T3` The signal $\mathbf{u}^* \in \mathbb{R}^{504}$ (Figure SM1, right) presents a smooth rounded feature, a narrow peak and a ramp. The same Gaussian blur of `T2` is used.

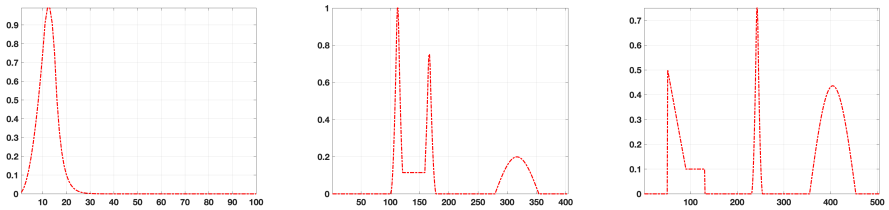

FIG. SM1. *1D test problems: ground truth* $\mathbf{u}^*$. *Left* `T1`*, center* `T2`*, right* `T3`.

*Supplementary material for SISC MS#M160094.
https://doi.org/10.1137/23M1600943

†Department of Civil, Chemical, Environmental, and Materials Engineering, University of Bologna, 40131 Bologna, Italy (villiam.bortolotti@unibo.it).

‡Department of Mathematics, University of Bologna, Piazza di Porta S. Donato 5, 40126 Bologna, Italy (germana.landi@unibo.it, fabiana.zama@unibo.it).

For these three test problems, we observe the behaviour of Algorithm UPenMM with $p = N$ penalty functions as follows:

(SM1.1)
$$\psi_i(\mathbf{u}) = (L\mathbf{u})_i^2 + \epsilon, \quad i = 1, \dots, N$$

where $L \in \mathbb{R}^{N\times N}$ is the discretization of the second order derivative operator and ϵ is a small positive constant in the range $[10^{-7}, 10^{-5}]$. Moreover, we analyse the generalized approach proposed in Algorithm GUPenMM with $\varepsilon = 0.9$, ψ_i as in (SM1.1) and the following generalized regularization parameter $\widetilde{\boldsymbol{\lambda}}$:

(SM1.2)
$$\widetilde{\lambda}_i = \frac{\|A\mathbf{u}_{\boldsymbol{\lambda}} - \mathbf{b}\|^2}{N\widetilde{\psi}_i(\mathbf{u}_{\boldsymbol{\lambda}})}, \quad \widetilde{\psi}_i(\mathbf{u}_{\boldsymbol{\lambda}}) = \max\{\psi_{i-1}(\mathbf{u}_{\boldsymbol{\lambda}}), \psi_i(\mathbf{u}_{\boldsymbol{\lambda}}), \psi_{i+1}(\mathbf{u}_{\boldsymbol{\lambda}})\},\ i = 1, \dots, N.$$

Both algorithms are tested in the unconstrained ($\Omega = \mathbb{R}^N$) and non-negatively constrained ($\Omega = \mathbb{R}^N_+$ where $\mathbb{R}^N_+$ is the positive orthant) cases. A solution of the subproblem at step 3 of Algorithms UPenMM and GUPenMM has been computed, in the unconstrained case, by solving its first order conditions, while the Newton Projection method [SM2] has been used in the constrained case.

The initial values $\boldsymbol{\lambda}_i^{(0)}$, $i = 1, \dots, N$, have been chosen such that

$$\boldsymbol{\lambda}_i^{(0)} = \frac{\|A\mathbf{b} - \mathbf{b}\|^2}{N\psi_i(\mathbf{b})} \quad \text{for Algorithm UPenMM;}$$
$$\boldsymbol{\lambda}_i^{(0)} = \frac{\|A\mathbf{b} - \mathbf{b}\|^2}{N\widetilde{\psi}_i(\mathbf{b})} \quad \text{for Algorithm GUPenMM.}$$

SM2. Low-noise results. We begin by analyzing the behaviour of the two algorithms in the case of low noise, both in the unconstrained ($\Omega = \mathbb{R}^N$) and in the non-negatively constrained ($\Omega = \mathbb{R}^N_+$) scenarios. To show the amount of noise on the blurred data we represent in Figure SM2 the blurred noisy data $\mathbf{b}$ (blue line), and the blurred data $\mathbf{y}$.

A first evaluation of the methods is made by inspecting the error history represented in Figure SM3(a) when $\Omega = \mathbb{R}^N$ and in Figure SM3(b) for $\Omega = \mathbb{R}^N_+$. Each picture shows the relative error curves of Algorithm UPenMM (black dash-dot line) and Algorithm GUPenMM (blue dashed line). The red dots represent the relative error values corresponding to the following `stopping criterion`:

(SM2.1)
$$\|\boldsymbol{\lambda}^{(k+1)} - \boldsymbol{\lambda}^{(k)}\| \le \|\boldsymbol{\lambda}^{(k)}\| Tol_\lambda$$

with $Tol_\lambda = 10^{-2}$. We can appreciate the positive influence of the modified evaluation of the regularization parameters introduced in Algorithm GUPenMM producing

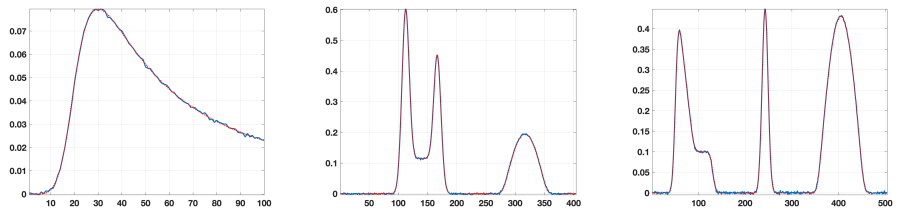

FIG. SM2. *1D test problems ($\delta = 0.01$). Blue line: blurred noisy data* $\mathbf{b}$*, dotted red line: blurred data* $\mathbf{y}$*. Left* `T1`*, center* `T2`*, right* `T3`.

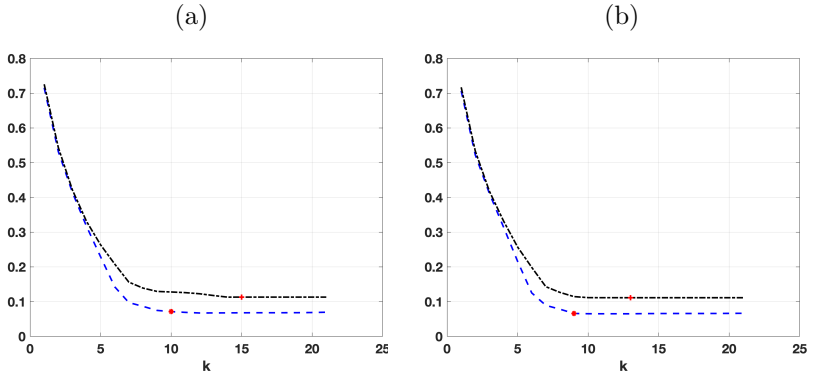

FIG. SM3. *Test problem* `T1` *($\delta = 0.01$). Relative error curves vs. the iteration index k. (a) Case $\Omega = \mathbb{R}^N$. (b) Case $\Omega = \mathbb{R}^N_+$. The black dash-dot line represents the relative error values of Algorithm UPenMM and the blue dashed line represents the relative error values of Algorithm GUPenMM. The red dots indicate the relative error values corresponding to stopping criterion* (SM2.1).

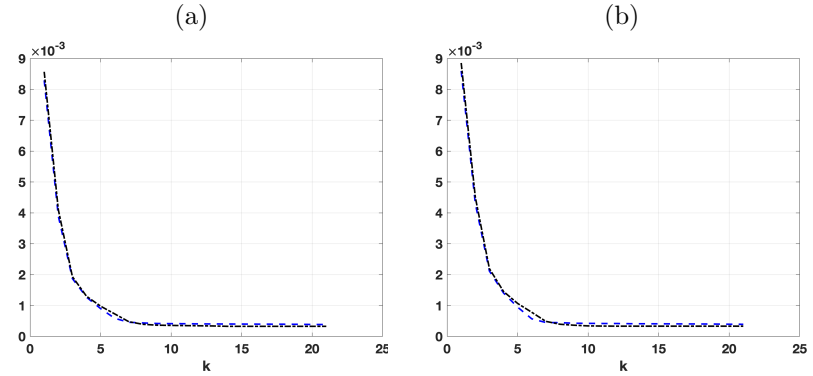

FIG. SM4. *Test problem* `T1` *($\delta = 0.01$). Value of the surrogate function. (a) $\Omega = \mathbb{R}^N$ (b) $\Omega = \mathbb{R}^N_+$. The black dash-dot line represents the $Q(\widehat{\boldsymbol{\lambda}}^{(k+1)}, \boldsymbol{\lambda}^{(k)})$ values in Algorithm UPenMM and the blue dashed line represents the $Q(\widetilde{\boldsymbol{\lambda}}^{(k+1)}, \boldsymbol{\lambda}^{(k)})$ values in Algorithm GUPenMM.*

smaller relative errors and faster convergence. The plot of the values of the surrogate function is shown in Figure SM4, demonstrating that the convergence criterion is met. The good agreement of the residual curves with the noise norm is observed in Figure SM5 where the black dash-dot line represents the residual norm values in Algorithm UPenMM and the blue dashed line indicates the residual norm values in Algorithm GUPenMM. The red line represents the noise norm. In addition to the error curves, the values in Table SM1 and the plots of the reconstructed signals in Figure SM6 confirm the superior quality obtained by Algorithm GUPenMM. This feature is even more evident in the case of more complex signals such as those represented by test problems T2 and T3; in these cases, we only represent the reconstructed signals for $\Omega = \mathbb{R}^N_+$ in Figure SM7. The computation times presented in Table SM2 show the performance of the different methods. The computation times for UPenMM and GUPenMM indicate a relatively stable increase across the test scenarios from T1 to T3. This increment is expected as the size of the test problems increases from T1 to T3. When the non-negativity constraint is present ("+" versions), computation

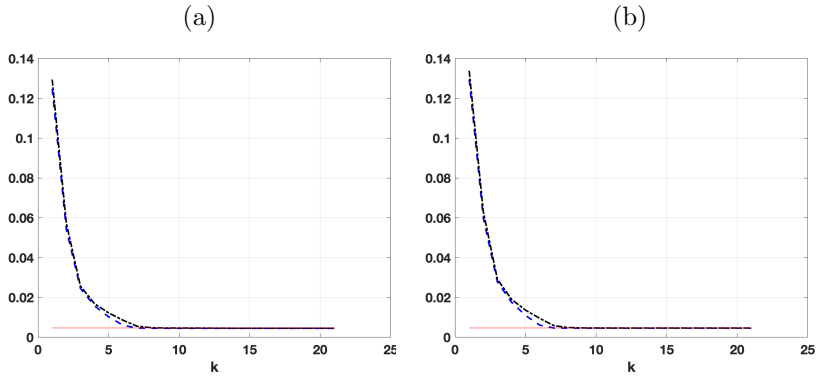

FIG. SM5. *Test problem* `T1` *($\delta = 0.01$). Behaviour of the residual norm. (a) $\Omega = \mathbb{R}^N$ (b) $\Omega = \mathbb{R}^N_+$. The black dash-dot line represents the residual norms in Algorithm UPenMM and the blue dashed line is the residual norms in Algorithm GUPenMM. The red line represents the noise norm.*

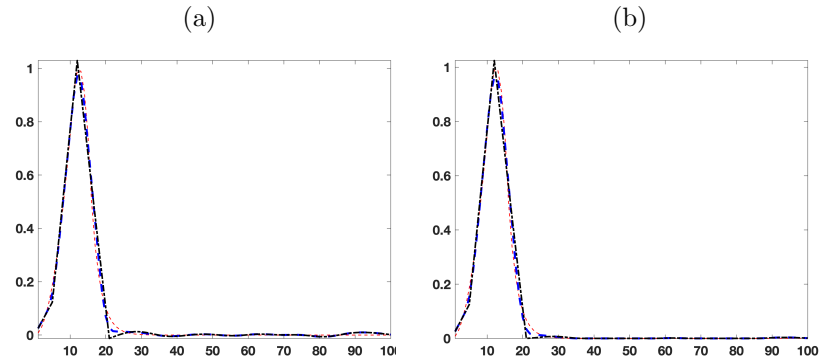

FIG. SM6. *Test problem* `T1` *($\delta = 0.01$). Solutions* $\mathbf{u}$*. (a) $\Omega = \mathbb{R}^N$ (b) $\Omega = \mathbb{R}^N_+$. The black dash-dot line represents* $\mathbf{u}$ *computed by Algorithm UPenMM and the blue dashed line represents* $\mathbf{u}$ *computed by Algorithm GUPenMM. The red dashed line represents the ground-truth solution.*

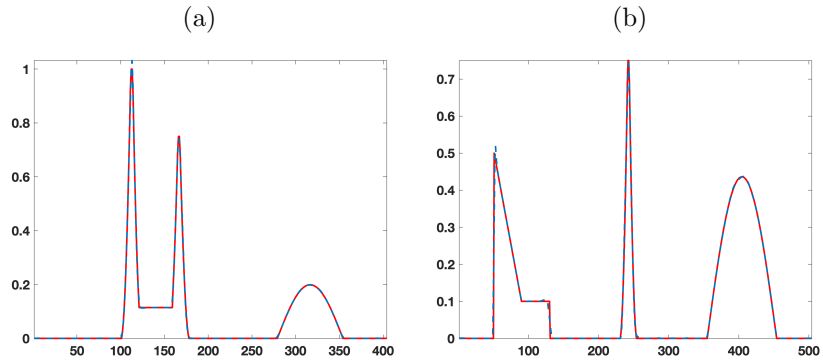

FIG. SM7. *Solutions* $\mathbf{u}$ *by Algorithm GUPenMM + (blue dashed line) and ground-truth solution (red dashed line). (a) Test problem* `T2` *($\delta = 0.01$) (b) Test problem* `T3` *($\delta = 0.01$).*

TABLE SM1

1D test problems ($\delta = 0.01$). Relative error and the corresponding number of iterations with $Tol_\lambda = 10^{-2}$. The symbol + indicates the constrained case. Between parenthesis, the number of Newton Projection iterations is reported.

Method	T1		T2		T3	
	Rel Err	Iters	Rel Err	Iters	Rel Err	Iters
UPenMM	$1.1313{\cdot}10^{-1}$	15	$9.8773{\cdot}10^{-2}$	7	$1.0532{\cdot}10^{-1}$	9
UPenMM +	$1.1136{\cdot}10^{-1}$	13(6)	$8.6412{\cdot}10^{-2}$	6 (42)	$1.0188{\cdot}10^{-1}$	11(47)
GUPenMM	$7.1381{\cdot}10^{-2}$	10	$2.5204{\cdot}10^{-2}$	7	$6.2736{\cdot}10^{-2}$	18
GUPenMM +	$6.5993{\cdot}10^{-2}$	9(48)	$2.7592{\cdot}10^{-2}$	9(66)	$6.1298{\cdot}10^{-2}$	19(65)
L2	$1.1527{\cdot}10^{-1}$	/	$7.9064{\cdot}10^{-2}$	/	$1.0380{\cdot}10^{-1}$	/
L2 +	$7.9265{\cdot}10^{-2}$	/	$6.1054{\cdot}10^{-2}$	/	$8.9234{\cdot}10^{-2}$	/

TABLE SM2

1D test problems ($\delta = 0.01$). Computation times in seconds. The symbol + indicates the constrained case.

Method	Computation times		
	T1	T2	T3
UPenMM	$3.01{\cdot}10^{-2}$	$5.53{\cdot}10^{-2}$	$1.09{\cdot}10^{-1}$
UPenMM +	$2.70{\cdot}10^{-2}$	$3.00{\cdot}10^{0}$	$2.75{\cdot}10^{0}$
GUPenMM	$2.75{\cdot}10^{-2}$	$1.66{\cdot}10^{-1}$	$3.06{\cdot}10^{-1}$
GUPenMM +	$2.78{\cdot}10^{-2}$	$3.00{\cdot}10^{0}$	$4.86{\cdot}10^{0}$

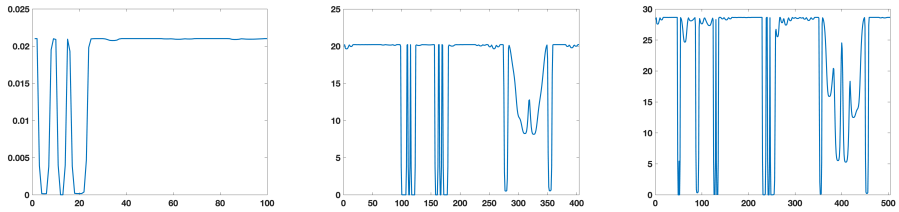

FIG. SM8. *1D test problems ($\delta = 0.01$). Regularization parameters computed by GUPenMM. Left* `T1`*, center* `T2`*, right* `T3`*.*

times for T2 and T3 increase in both UPenMM+ and GUPenMM+. Despite this increase, Table SM1 shows that the accuracy generally improves. This suggests that the non-negativity constraint, while increasing computation time, enhance the solution's precision. A final consideration concerns the values of the point-wise regularization parameters. Figure SM8 illustrates the characteristic of this method: since all the penalty terms are constant, then the values of the regularization parameters are larger in correspondence with flat areas and become smaller where the solution exhibits rapid changes. The last two rows of Table SM1 compare the relative errors when utilizing the Tikhonov method with optimal regularization parameter. Figure SM9 illustrates that a single parameter, even if optimally weighted, is unable to reconstruct equally well all the details of complex signals presenting many different features (e.g. `T2`, `T3`).

SM3. High-noise results. In this section, we present the results obtained with high-noise ($\delta = 0.1$), restricted to the case $\Omega = \mathbb{R}^N_+$, because the absence of the non-negativity constraint produces worse results. Figure SM10 shows the blurred noisy

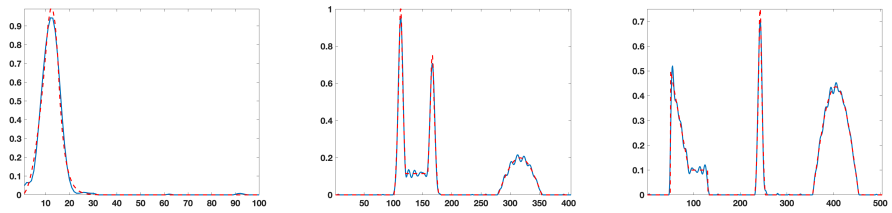

FIG. SM9. *1D test problems ($\delta = 0.01$). Method L2+ with optimal regularization parameter. Left* `T1`*, $\lambda = 2.7838 \times 10^{-5}$. Center* `T2`*, $\lambda = 3.495495 \times 10^{-3}$. Right* `T3`*, $\lambda = 3.242424 \times 10^{-3}$.*

data $\mathbf{b}$ (blue line), and the blurred data $\mathbf{y}$.

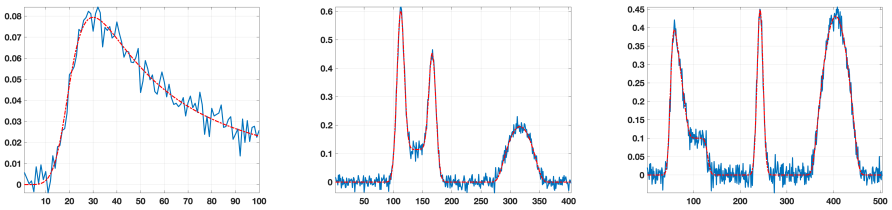

FIG. SM10. *1D test problems ($\delta = 0.1$). Blue line: blurred noisy data $\mathbf{b}$, dashed red line: blurred data $\mathbf{y}$. Left* `T1`*, center* `T2`*, right* `T3`*.*

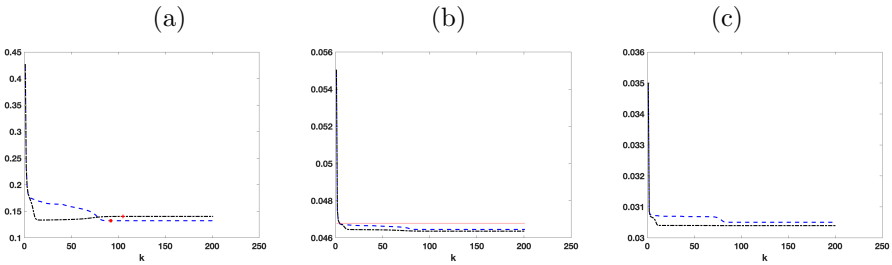

FIG. SM11. *T1 test problem ($\delta = 0.1$). (a) Relative error curves: Algorithm UPenMM (black dash-dot line) and Algorithm GUPenMM (blue dashed line). Red dots indicate values at the exit criterion* (SM2.1)*. (b) Residual norm behaviour: Algorithm UPenMM (black dash-dot line), Algorithm GUPenMM (blue dashed line), and noise norm (red line). (c) Surrogate function values: $Q(\widehat{\boldsymbol{\lambda}}^{(k+1)}, \boldsymbol{\lambda}^{(k)})$ for Algorithm UPenMM (black dash-dot line) and $Q(\widetilde{\boldsymbol{\lambda}}^{(k+1)}, \boldsymbol{\lambda}^{(k)})$ for Algorithm GUPenMM (blue dashed line).*

In Figure SM11(a), we represent the relative error curves of Algorithm UPenMM (black dash-dot line) and Algorithm GUPenMM (blue dashed line) for T1. The red dots represent the relative error values corresponding to the `stopping criterion` (SM2.1) with $Tol_\lambda = 10^{-5}$. Compared to the low-noise case, a smaller value of the tolerance is necessary to stop the algorithms close to their limit. While the error of Algorithm UPenMM decreases more rapidly in the initial iterations, Algorithm GUPenMM achieves a slightly smaller error in the limit. The good agreement of the residual curves with the noise norm is observed in Figure SM11(b) where the black dash-dot line represents the residual norm values in Algorithm UPenMM, the blue dashed line indicates the residual norm values in Algorithm GUPenMM and the red

TABLE SM3

1D test problems ($\delta = 0.1$). Relative error and the corresponding number of iterations with $Tol_\lambda = 10^{-5}$. The symbol + indicates the constrained case. Between parenthesis, the number of Newton Projection iterations is reported.

Method	T1		T2		T3	
	Rel Err	Iters	Rel Err	Iters	Rel Err	Iters
UPenMM +	$1.401{\cdot}10^{-1}$	105(169)	$1.081{\cdot}10^{-1}$	14(72)	$1.093{\cdot}10^{-1}$	15(89)
GUPenMM +	$1.323{\cdot}10^{-1}$	92(171)	$8.068{\cdot}10^{-2}$	84(241)	$1.072{\cdot}10^{-1}$	361(825)
L2 +	$1.427{\cdot}10^{-1}$	/	$1.019{\cdot}10^{-1}$	/	$1.270{\cdot}10^{-1}$	/

TABLE SM4

1D test problems ($\delta = 0.1$). Computation times in seconds. The symbol + indicates the constrained case.

Method	Computation times		
	T1	T2	T3
UPenMM +	$5.61{\cdot}10^{-2}$	$3.02{\cdot}10^{0}$	$5.58{\cdot}10^{0}$
GUPenMM +	$7.57{\cdot}10^{-2}$	$9.36{\cdot}10^{0}$	$4.50{\cdot}10^{1}$

line represents the noise norm. The plot of the values of the surrogate function is shown in Figure SM11(c). Figure SM12(a) shows the good reproduction of the high

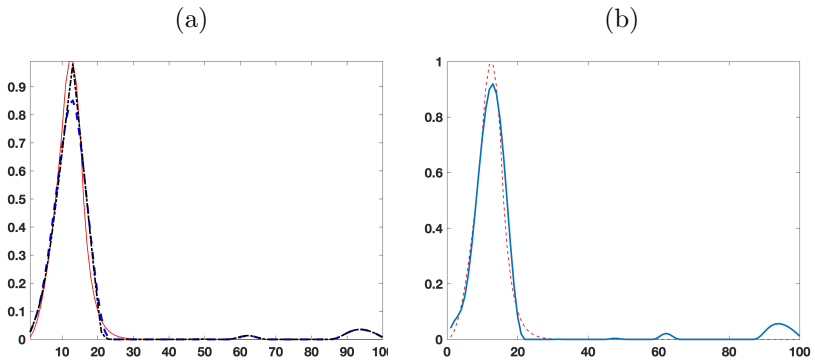

FIG. SM12. *Test problem* T1 *($\delta = 0.1$). Solution* $\mathbf{u}$ *with* $\Omega = \mathbb{R}^N_+$. *(a)* $\mathbf{u}$ *computed by Algorithm UPenMM (black dash-dot line),* $\mathbf{u}$ *computed by Algorithm GUPenMM (blue dashed line) and ground-truth solution (red dashed line). (b) Solution computed by Tikhonov L2+ (blue line) with optimal parameter $\lambda = 1.5167\ 10^{-3}$, and ground-truth solution (red dashed line).*

peak obtained from both algorithms, with spurious oscillations in the flat region that, however, they are less pronounced compared to the Tikhonov $L2+$ solution with optimal regularization parameter (Figure SM12(b)). A similar behaviour is observed in tests T2 and T3, as depicted in Figures SM13 and SM14. Table SM3 shows that the smallest relative error is obtained by Algorithm GUPenMM (row GUPenMM +) in each case and that Tikhonov $L2+$ produces the worst results. Figure SM15 represents the point-wise regularization parameter, confirming the characteristics already observed in the low-noise case. Finally, concerning the computation times reported in Table SM4, we observe higher values compared to the low-noise case (Table SM2) due to the use of a smaller tolerance ($Tol_\lambda = 10^{-5}$ *vs* $Tol_\lambda = 10^{-2}$ with low noise). Additionally, GUPenMM + is more expensive compared to UPenMM +.

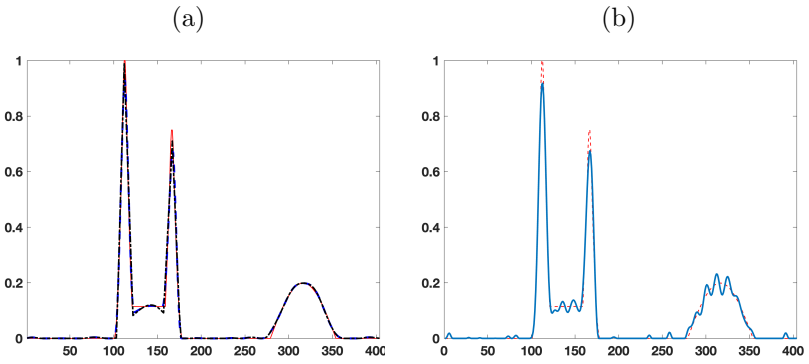

FIG. SM13. *Test problem* `T2` *($\delta = 0.1$). Solution* $\mathbf{u}$ *with* $\Omega = \mathbb{R}^N_+$. *(a)* $\mathbf{u}$ *computed by Algorithm UPenMM (black dash-dot line),* $\mathbf{u}$ *computed by Algorithm GUPenMM (blue dashed line) and ground-truth solution (red dashed line). (b) Solution computed by Tikhonov L2+ (blue line) with optimal parameter* $\lambda = 7.2326\ 10^{-2}$, *and ground-truth solution (red dashed line).*

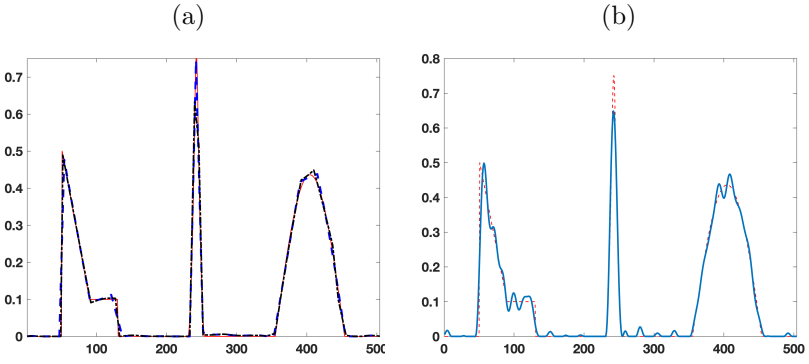

FIG. SM14. *Test problem* `T3` *($\delta = 0.1$). Solution* $\mathbf{u}$ *with* $\Omega = \mathbb{R}^N_+$. *(a)* $\mathbf{u}$ *computed by Algorithm UPenMM (black dash-dot line),* $\mathbf{u}$ *computed by Algorithm GUPenMM (blue dashed line) and ground-truth solution (red dashed line). (b) Solution computed by Tikhonov L2+ (blue line) with optimal parameter* $\lambda = 6.0103\ 10^{-1}$, *and ground-truth solution (red dashed line).*

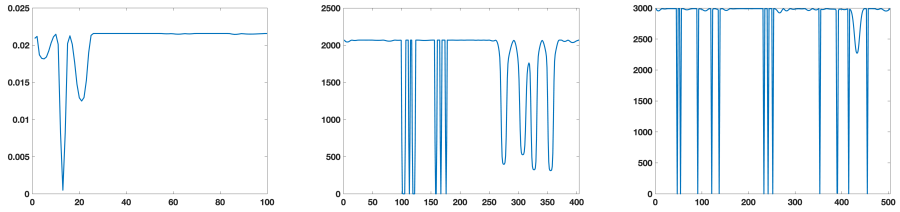

FIG. SM15. *1D test problems ($\delta = 0.1$). Regularization parameters computed by GUPenMM. Left* `T1`, *center* `T2`, *right* `T3`.

REFERENCES

[SM1] P. C. HANSEN, *Regularization tools version* 4.0 *for Matlab* 7.3, Numerical algorithms, 46 (2007), pp. 189–194.

[SM2] D. BERTSEKAS, *Nonlinear Programming*, Athena Scientific, (2nd Edition), 1999.